Supporting Information

A strategy of electrochemical simultaneous detection of acetaminophen and levofloxacin in water based on g-C_3N_4 nanosheets doped graphene oxide

Wenwen Yi, [a] Chunxiao Han, [a] Zhongping Li, *[a] Yujing Guo, *[a] Meng Liu [b] and Chuan Dong [a]

[a] *Institute of Environmental Science, Shanxi University, Taiyuan 030006, P.R. China.*

[b] *School of Environmental Science and Technology, Key Laboratory of Industrial Ecology and Environmental Engineering (Ministry of Education), Dalian University of Technology, Dalian 116024, China.*

**Corresponding author:* Zhongping Li, Yujing Guo

Email address: zl104@sxu.edu.cn (Z.P. Li)

guoyj@sxu.edu.cn（Y.J. Guo）

1. Reagents and apparatus

Melamine ($C_3N_3(NH_2)_3$), Levofloxacin ($C_{18}H_{20}FN_3O_4$), Na_2HPO_4, NaH_2PO_4 were purchased from Aladdin Reagent Co.,Ltd (Shanghai, China), graphite powder was supplied from Tianjin Reagent Factory. Paracetamol ($C_8H_9NO_2$) was purchased from Macklin Biochemical Co.,Ltd (Shanghai, China). All other reagents used in the experiment were analytical reagents. Ultrapure water (18.2 MΩ, Millipore) was used throughout all the experiments.

Scanning electron microscope (SEM) images and transmission electron microscopy (TEM) were recorded on JEM–2010 (JEOL, Japan) and JEM–2100, respectively, for the characterization of materials. Photoluminescence spectra were obtained on a Model FP-8300 spectrometer (JASCO, Japan) with both emission and excitation slits setting at 5 nm. UV–vis spectra were carried out on a Perkin Elmer, Lambda 950 UV–Vis spectrophotometer. X–ray diffraction (XRD) patterns were measured with a D8 advanced X–ray diffractometer (Bruker AXS, Germany). X-ray photoelectron spectroscopy (XPS) of as-prepared samples was acquired using a Thermo ESCA LAB spectrometer (USA). The Fourier transform infrared (FT-IR) spectra were obtained on TENSOR II infrared spectrometer (Bruker Germany). All electrochemical measurements were carried out on a traditional three-electrode system using a CHI660E electrochemical work-station (Shanghai Chenhua Instrument company, China) with the as-prepared materials covered GCE or bare GCE (3 mm in diameter) as the working electrodes, a Pt wires as the auxiliary electrode, and a saturated Ag/AgCl (saturated KCl) as reference electrode.

2. Synthesis of GO, CNNS and CNNS/GO

The synthesis of graphite oxide is in the light of the modified Hummers' method.[1] The synthesis process of graphitic carbon nitride nanosheets (CNNS) comprised two steps. (1) Bulk g-C_3N_4 was synthesized by pyrolysis method. Briefly, 5 g melamine was heated at 550°C for 2 h under an atmospheric environment with a heating rate of 2°C min^{-1}.

The resultant agglomerates were ground for powder, then further heated at 540°C for 4 h. (2) CNNS was synthesized by ultrasound-assisted method. The yellow powder was dispersed in distilled water and then ultrasound for more than 10 hours constantly. Then initial formed white suspension was centrifuged at 4500 rpm to clear away the residual unpeeled g-C_3N_4. Bulk g-C_3N_4 and CNNS were collected and used for further researches. (Fig. S1)

Preparation of CNNS/GO composite:

1 mg/mL CNNS suspension was added 1 mg/mL GO aqueous solution with ultrasound. In this experiment, the same method was used to synthesize composite materials with different mass ratios (CNNS:GO mass ratios 1:1，3:1，5:1，7:1).

(a) Bulk g-C_3N_4 (b) CNNS

Fig. S1 Visual appearance of (a) Bulk g-C_3N_4 and (b) CNNS.

3. Construction of electrochemical sensor

Before the preparation, the bare GCE surface was polished with 0.05 μm alumina microparticles and rinsed carefully with ultrapure water and ethyl alcohol, until get a mirrored surface. Then 8.0 μL of as-prepared CNNS/GO composite (1 mg mL^{-1}) dispersion was coated on the surface of the GCE to obtain the CNNS/GO/GCE and then dried under an infrared lamp. CNNS/GCE and GO/GCE were fabricated using the above method as a control electrode. And all experiments were carried out at room temperature.

4. Electrochemical experiments

All electrochemical measurements were investigated in 0.1 M PBS solution (pH 5.0) by differential pulse voltammetry (DPV) or cycle voltammetry (CV). The electrochemical impedance spectroscopy (EIS) measurements were performed in 0.1 M KCl containing 5.0 mM $K_3[Fe(CN)_6]$/K_4 $[Fe(CN)_6]$and recorded between 0.1 Hz and

100 KHz with a sinusoidal voltage perturbation of 5 mV amplitude.

5. Results and discussion

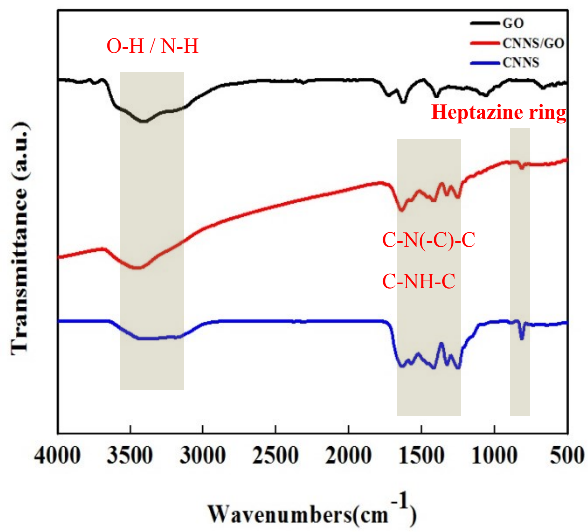

Fig. S2 FT-IR spectrum of GO, CNNS/GO, CNNS

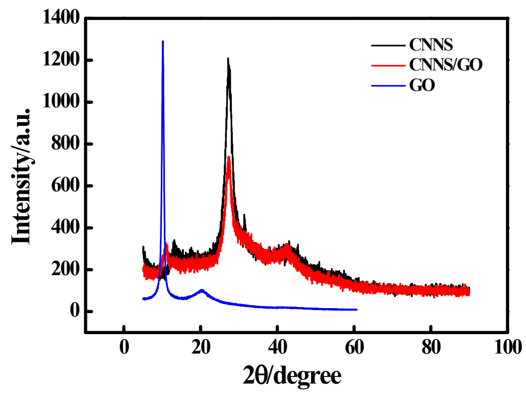

Fig. S3 XRD of CNNS, CNNS/GO and GO.

X-ray diffraction (XRD) spectra were used to determine the crystal structure of as-prepared materials. As revealed in Fig. S3, the graphite-like phase nitride carbon nanosheet (CNNS) had a typical features strong peak at 27.36° , which is due to the interplanar stacking of aromatic C–N heterocycles present in CNNS and a broad peak at 13.07° . The peak at 2θ = 13.07° derives from the in-planar repeated tri-s-triazine units.[2,3] The GO had an obvious characteristic sharp peak at 10.2° . In addition, the CNNS/GO composite had a broad peak at 10.97° and a sharp peak at 27.22° . These results demonstrated that CNNS and GO forming CNNS/GO composite via chemical bonds.[4]

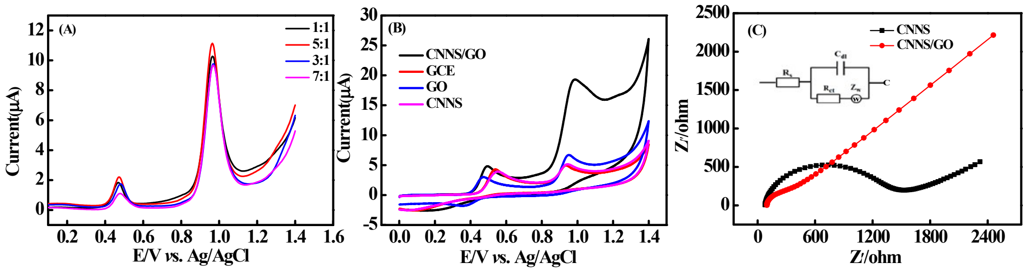

Fig. S4 (A) The DPV peak current of different mass ratio of CNNS and GO (1:1, 3:1, 5:1, 7:1) in the solution of AC and LEV. (B) The CV response of different electrodes with the presence of AC (50 μM) and LEV (25 μM) containing 0.1 M PB solution (pH 5.0) at scan rate of 100 mV s^{-1}. (C) EIS of different electrodes (CNNS/GCE, CNNS/GO/GCE) in 5.0 mM $[Fe(CN)_6]^{3-/4-}$ solution containing 0.1 M KCl and the Randles equivalent circuit model (inset).

Fig. S4 (C): In the equivalent circuit diagram, R_{et} is the charge transfer the resistance that reflects the blocking behavior of the electrode interface, C is the differential capacitance, Z_w is the Warburg impedance, and R_s is Solution phase resistance.

Table S1 Values of the equivalent circuit parameters of the fitting curves for the CNNS/GCE and CNNS/GO/GCE

	R_s(ohm)	C（F）	R_{et} (ohm)	W(S · sec^5)
CNNS/GCE	82.6	$5.35E^{-7}$	1224.1	0.0009655
CNNS/GO/GCE	87.9	$7.14E^{-7}$	152.3	0.0002100

The current responses of different electrodes

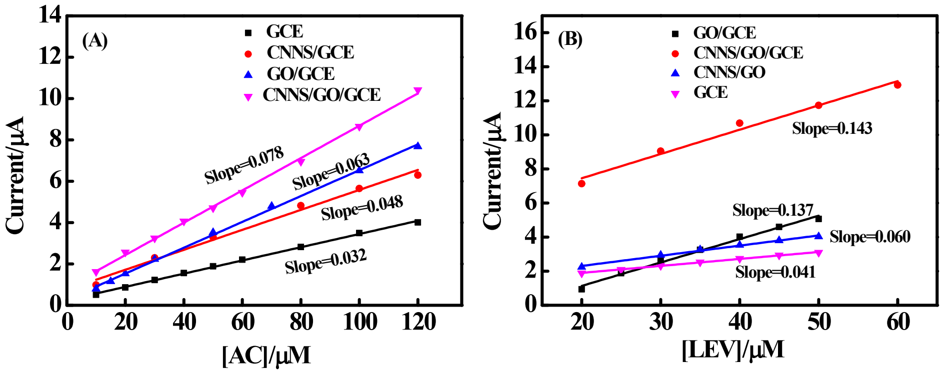

Fig.S5 The linear fitting plot of oxidation current responses value of different electrodes (GCE, CNNS/GCE, GO/GCE, CNNS/GO/GCE) vs. AC (A) or LEV (B) concentration.

A similar result of the electrodes is obtained in this test. In Fig. S5(A) and (B), it is worth noting that the response of the CNNS/GO sensor is apparently higher than other sensors in every tested concentration. Additionally, according to the linear fitting plot of oxidation current responses value of different electrodes with AC or LEV concentration, it can be known that the slope of CNNS/GO/GCE is the largest, indicating that the sensor has a higher sensitivity than other electrodes.

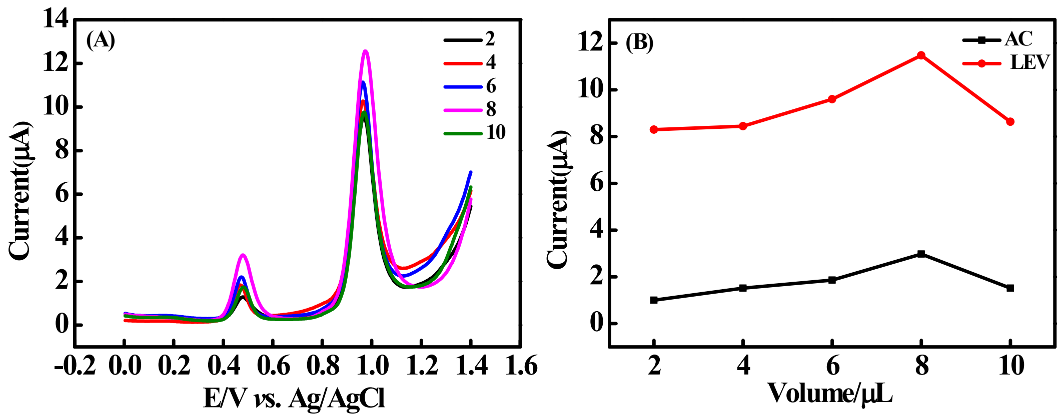

Fig. S6 (A) The CV response of different electrode modification amount with the presence of AC (50 μM) and LEV (25 μM) containing 0.1 M PB solution (pH 5.0) at scan rate of 100 mV s^{-1}. (B) Ip vs. modifier amount plots for AC and LEV.

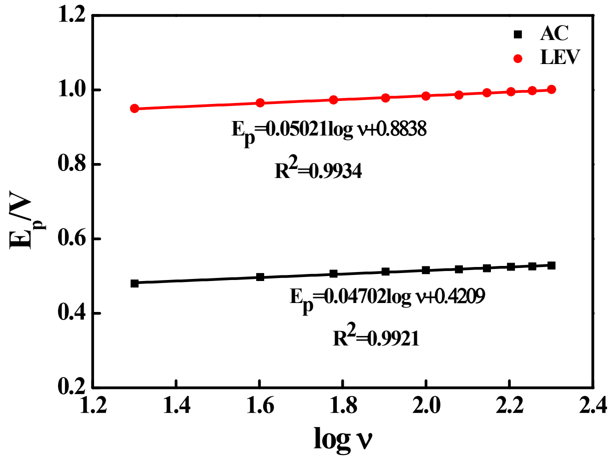

Fig. S7 Plot of the peak potential versus the logarithm of scan rate (0.1 M PBS, pH 5.0, AC (50 μmol L^{-1}) and LEV (25 μmol L^{-1})).

$$E_{pa} = \boldsymbol{E}^{0'} + [2.303\ R\ T/(1- \alpha\ )\ n_{\alpha}\ F]\ \log \nu + \text{constant} \qquad (1)$$ [5]

where $E^{0'}$ indicates the formal potential, ν is the scan rate (mV s^{-1}); α is the electron transfer coefficient; F, T, and R are Faraday's constant, the temperature, and the universal gas constant, respectively.[6] n_{α} is the electron number involved in the rate determining step;

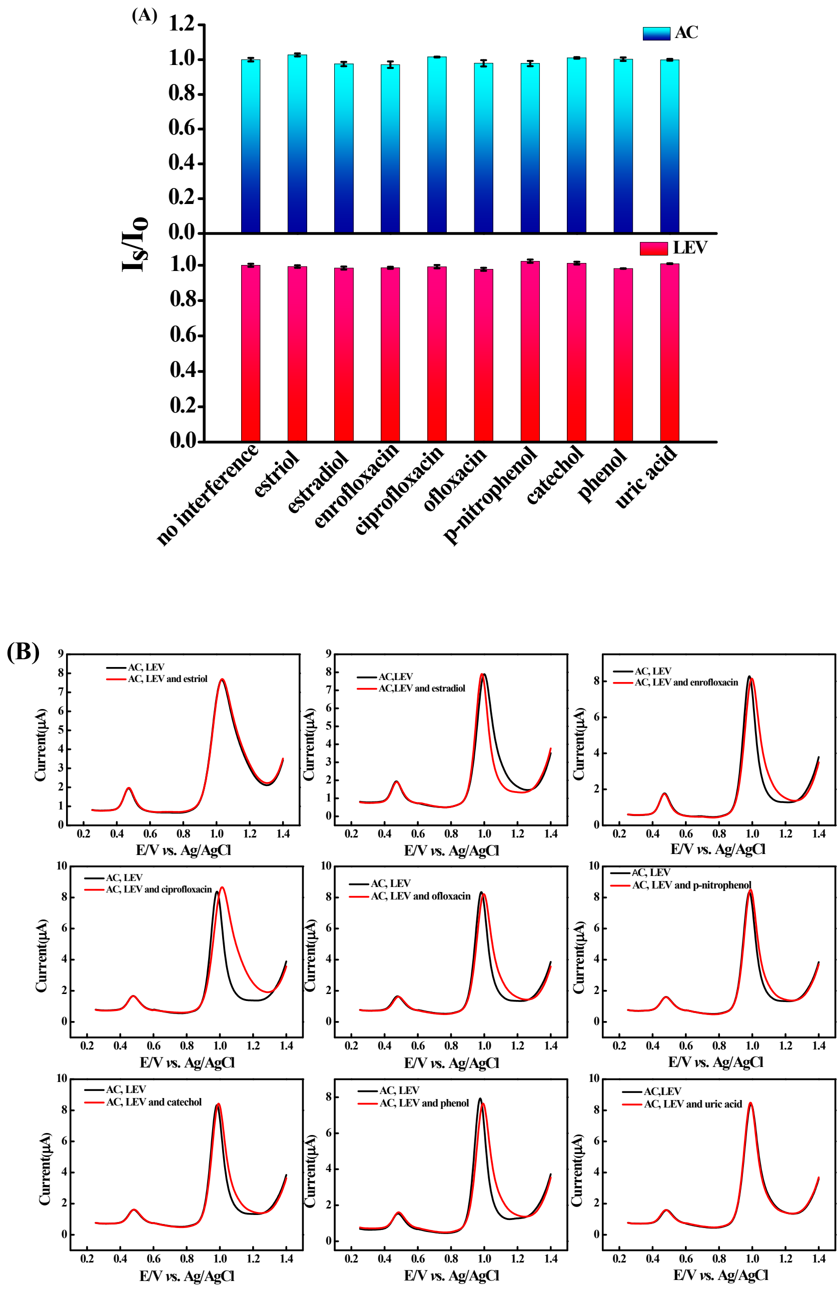

Fig. S8 (A) Current responses of AC (50 μM) and LEV (25 μM) in the presence and absence of 250 μM interfering substances in 0.1 M phosphate buffer (pH 5.0) at CNNS/GO/GCE. (B) The corresponding voltammograms obtained in interference studies.

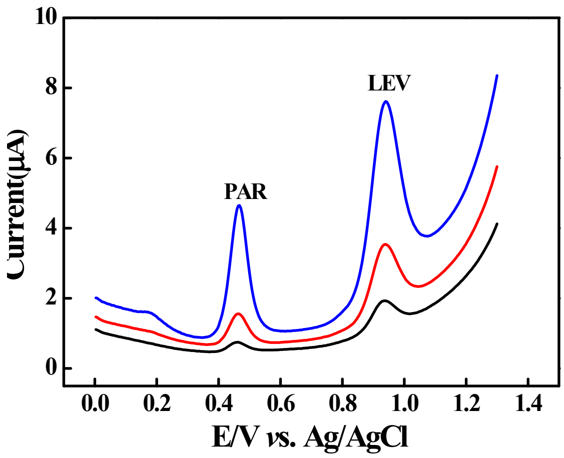

Fig. S9 DPV response for AC and LEV in river water samples using CNNS/GO/GCE.

Compared with previous report

Table S2. Comparison of the various modified electrodes for electrochemical determination of AC or LEV.

Analyte	Electrode	Methods	Linear range/μM	LOD/μM	Ref.
AC	Sl-CPE	DPV	1-160	0.021	7
	P-RGO/GCE	DPV	1.5-120	0.36	8
	NiO/CNTs/DPID/CPE	DPV	0.8-550	0.3	9
	SnO2@MWCNT/β-CD	DPV	0.01 – 340	5.8	10
	Polyimide-MWCNT	DPV	2-1800	2	11
	Fe_2O_3/RGO	DPV	0.1-74	0.021	12
	AgNPs-CB-PEDOT:PSS/GCE	SWV	0.62-7.1	0.012	13
	MWCNTs/poly(Gly)/GCE	DPV	0.5-10	0.45	14
	CNNS/GO/GCE	DPV	0.5-1000	0.0147	This work
LEV	CuNPs/rGO/GCE	DPV	0.1-2.5	0.017	15
	SbNPs/rGO/GCE	DPV	0.2-4	0.041	15
	PoAP/MWCNTs/GCE	DPV	3.0-200	3.3	16
	NiO–AgNPs/GCE	SWV	0.25-100	0.027	17
	MIP/G–AuNPs/GCE	DPV	1-100	0.53	18
	Au/ssDNA/SWCNTs	SWV	1-10	0.075	19
	AgNPs-CB-PEDOT:PSS/GCE	SWV	0.67-12	0.014	13
	Azure-B/PGE	DPV	2-125	1.2	20
	CNNS/GO/GCE	DPV	0.25-90	0.073	This work

Sample analysis

Table S3 Simultaneous determination of AC and LEV in river water sample with the electrochemical sensor.

Sample			Sensor						HPLC					
	Add (μM)		Found (μM)		Recovery (%)		RSD (%)		Found (μM)		Recovery (%)		RSD (%)	
	AC	LEV	AC	LEV	AC	LEV	AC	LEV	AC	LEV	AC	LEV	AC	LEV
River water	0		Undetected						Undetected					
	0.8	1	0.82	1.09	102.5	109.0	2.56	3.40	0.79	0.98	98.8	98.0	1.03	2.45
	5	3	5.59	2.94	111.8	98.0	1.33	3.85	4.87	3.10	97.4	103.3	3.20	3.80
	28	10	28.11	9.56	100.4	95.6	3.9	5.01	28.2	10.2	100.7	102	1.55	3.19

References

1. Z. H. Sheng, L. Shao, J. J. Chen, W. J. Bao, F. B. Wang and X. H. Xia, Catalyst–free synthesis of nitrogen–doped graphene via thermal annealing graphite oxide with melamine and its excellent electrocatalysis, ACS Nano, 2011, **5**, 4350–4358.
2. M. Rakibuddin and H. Kim, Reduced graphene oxide supported C_3N_4 nanoflakes and quantum dots as metal-free catalysts for visible light assisted CO_2 reduction, Beilstein J. Nanotechnol, 2019, **10**, 448–458.
3. B. H. Qu, Z. Y. Mu, Y. L, Y. S. Liu, R. Yan, J. H. Sun, Z. S. Zhang, P. Li and L. Q. Jing, The synthesis of porous ultrathin graphitic carbon nitride for the ultrasensitive fluorescence detection of 2,4,6-trinitrophenol in environmental water, Environ. Sci.:Nano, 2019, **6**, 207.
4. H. Zhang, Y. Huang, S. Hu, Q. Huang, C. Wei, W. Zhang, L. Kang, Z. Huang and A. Hao, Fluorescent probes for off-on sensitive and selective detection of mercury ions and L-cysteine based on graphitic carbon nitride nanosheets. J. Mater. Chem. C, 2015, **3**, 2093–2100.

5. A. Sudarvizhi, K. Pandian, O. S. Oluwafemi and S. C. B. Gopinath, Amperometry detection of nitrite in food samples using tetrasulfonated copper phthalocyanine modified glassy carbon electrode, Sens. Actuators B Chem., 2018, **272**, 151–159.

6. Y. J. Han, R. Zhang, C. Dong, F. Q. Cheng and Y. J. Guo, Sensitive electrochemical sensor for nitrite ions based on rose-like AuNPs/MoS_2/graphene composite, Biosens. Bioelectron., 2019, **142**, 111529.

7. N. P. Shetti, S. J. Malode, D. S. Nayak, K. RaghavaReddy, Ch. VenkataReddy and K. Ravindranadh, Silica gel-modified electrode as an electrochemical sensor for the detection of acetaminophen, Microchem. J., 2019, **150**, 104206.

8. X. Zhang, K. P. Wang, L. N. Zhang, Y. C. Zhang and L. Shen, Phosphorus-doped graphene-based electrochemical sensor for sensitive detection of acetaminophen, Anal. Chim. Acta, 2018, **1036**, 26-32

9. H. Karimi-Maleh , M. R. Ganjali and P. Norouzi, Amplified nanostructure electrochemical sensor for simultaneous determination of captopril, acetaminophen, tyrosine and hydro- chlorothiazide, Mat. Sci. Eng. C, 2017, **73**, 472-477.

10. R. K. Deviab, G. Muthusankara, G. Gopua, L. J. Berchmans, A simple self-assembly fabrication of tin oxide nanoplates on multiwall carbon nanotubes for selective and sensitive electrochemical determination of antipyretic drug, Colloid. Surface. A, 2020, **598**, 124825.

11. M. Burç, S. Köytepe, S. T. Duran, N. Ayhan, B. Aksoy, T. Seçkin, Development of voltammetric sensor based on polyimide-MWCNT composite membrane for rapid and highly sensitive detection of paracetamol, Measurement, 2020, **151**, 107103.

12. V. N. Palakollu, T. E. Chiwunze, C. Liu and R. Karpoormath, Electrochemical sensitive determination of acetaminophen in pharmaceutical formulations at iron oxide/graphene composite modified electrode, Arab. J. Chem., 2019 .

13. A. Wong, A. M. Santos and O. Fatibello-Filho, Simultaneous determination of paracetamol and levofloxacin using a glassy carbon electrode modified with carbon black,silver nanoparticles and PEDOT:PSS film, Sens. Actuator B Chem., 2018, **255**, 2264–2273.

14. P. V. Narayana, T. M. Reddy, P. Gopal and G. R. Naidu, Electrochemical sensing of par-acetamol and its simultaneous resolution in the presence of dopamine and folic acid at a multi-walled carbon nanotubes/poly(glycine) composite modified electrode. Anal. Methods, 2014,

6, 9459-9468.

15. K. L. Martin, D. Silva, R. P. Simo˜es and I. Cesarino, Evaluation of reduced graphene oxide modified with antimony and copper nanoparticles for levofloxacin oxidation. Electroanal., 2018, **30**, 2066–2076.
16. W. Wen, D. M. Zhao, X. H. Zhang, H. Y. Xiong, S. F. Wang, W. Chen and Y. D. Zhao, One-step fabrication of poly(o-aminophenol)/multi-walled carbon nanotubes composite film modified electrode andits application for levofloxacin determination in pharmaceuticals, Sens. Actuator B Chem., 2012, **174**, 202–209.
17. C. Q. Liu, D. Xie, P. Liu, S. L. Xie, S. S. Wang, F. L. Cheng, M. Zhang and L. S. Wang, Voltammetric determination of levofloxacin using silver nanoparticles deposited on a thin nickel oxide porous film, Microchim. Acta, 2019, **186**, 21.
18. F. Wang, L. hua, Z. Jing and D. Zhang, Electrochemical sensor for levofloxacin based on molecularly imprinted polypyrrole–graphene–gold nanoparticles modified electrode, Sens. Actuator B Chem., 2014, **192**, 642-647.
19. F. C. Moraes, T. A. Silva and I. Cesarino, Antibiotic detection in urine using electrochemical sensors based on vertically aligned carbon nanotubes, Electroanalysis, 2013, **25**, 2092-2099.
20. M. M. Vinay, Y. Arthoba Nayaka, R. O. Yatisha, K. V. Basavarajappa, P. Manjunatha and H. T. Purushothama, Development of Azure-B modified pencil graphite electrode as an electrochemical sensor for the investigation of Levofloxacin in pharmaceutical and biological samples, chem. Date. collect., 2020, **28**, 100441–100448.